Acta Geodyn. Geomater., Vol. 21, No. 1 (213), 99–110, 2024
DOI: 10.13168/AGG.2024.0009
journal homepage: https://www.irsm.cas.cz/acta

ORIGINAL PAPER

DIFFERENCES IN STRENGTH, SEEPAGE, AND ACOUSTIC EMISSION CHARACTERISTICS OF RAW COAL AND BRIQUETTE COAL SAMPLES : A TRIAXIAL COMPRESSION EXPERIMENT INVESTIGATION

Baokun ZHOU [1], Erhui ZHANG [2] *, Xukai DONG [1], Changfeng LI [1] and Ping LI [3]

[1] *School of Energy and Mining Engineering, China University of Mining and Technology Beijing, Beijing 100083, China*
[2] *School of Emergency Management and Safety Engineering, China University of Mining and Technology Beijing, Beijing 100083, China*
[3] *School of Management and Engineering, Capital University of Economics and Business, Beijing 100071, China*

**Corresponding author's e-mail:* 1440805440@qq.com

ARTICLE INFO

Article history:
Received 31 October 2023
Accepted 4 March 2024
Available online 2 April 2024

Keywords:
Raw coal and briquettes coal
Triaxial experiment
Strength characteristics
Acoustic emission
Seepage; Stress sensitivity
Seepage
Sensitivity

ABSTRACT

The differences in intensity, acoustic emission (AE), and seepage characteristics between raw coal and briquette coal were studied under a triaxial compression experiment. The two stress-strain curves of raw coal and briquette coal had similar trends and could be divided into five development stages in the triaxial compression experiment. The transverse and axial deformations of briquette coal were larger than those of raw coal, and the compressive strength and elastic modulus of briquette coal were smaller than those of raw coal. The cumulative AE count and energy of the whole compression process of raw coal were higher than that of briquette coal. The seepage velocities of gases increased with the deformation and failure of coal samples, and its variation trend corresponded to the failure stage of coal samples. Their permeability velocity was small at the initial stage of raw coal and briquette coal. However, the maximum permeability velocity of briquette coal was much higher than that of raw coal after the failure of coal samples. Both raw coal and briquette coal had strong stress sensitivity. The permeability of the two types of samples decreased exponentially with the increased effective stress. The seepage velocity of briquette coal was most sensitive to axial force and deformation, while that of raw coal was more sensitive to radial deformation. The research results provide references for the experimental study of using briquette coal instead of raw coal as well as for exploring coal and gas outburst mechanisms in coal seam.

1. INTRODUCTION

Coal as important fossil energy ensures national energy security. As China's main energy source, its status will not change for a long period (Wei et al., 2012; Fu et al., 2020). Coal mining has gradually turned to deep mining due to the large demand for coal resources in China and decreased shallow resources. Deep mining conditions are complex. The frequency and intensity of coal and gas outbursts increase, which seriously threatens the safety production of coal mines and the personal safety of staff (Mark et al., 2016; Peng et al., 2012; Liu et al., 2022).

Considerable amounts of coal and gases may be violently ejected in the coal and gas outburst process (Wu et al., 2020). Methane is the main component of coal seam gases, and the greenhouse effect of methane is 28 times that of carbon dioxide (Zhang et al., 2023). A large amount of methane emitted in the coal and gas outburst aggravates the greenhouse effect (Wang et al., 2021). Therefore, the strength, seepage, and AE characteristics of coal are studied. It is of great significance to the monitoring and prevention of coal and gas outburst accidents and environmental protection.

Raw coal and briquette coal are used as samples in the experimental research of coal and gas outbursts. Most coal seam in coal mines are relatively soft, so it is difficult to make standard experimental samples of raw coal. More and more experiments used briquette coal as research objects (Zhang et al., 2020; Ge et al., 2022). The formation of briquette coal typically involves the blending of pulverized coal with water and subsequent compression using a specialized mold. This process facilitates convenient processing and shaping. However, compared with raw coal, briquette coal damaged the original coal structure. Its physical and mechanical properties change, which leads to the controversy on the feasibility of replacing raw coal with briquette coal in experiments (Zhou et al., 2022; Li et al., 2017; Cao et al., 2010).

Researchers have studied the differences in strength and seepage characteristics of raw coal and briquette coal. Cao et al. (2010) used the self-developed triaxial seepage device to test briquette coal and raw coal. The full stress-strain curves of the two types of coal samples can be divided into five stages, with a corresponding relationship between the seepage velocity and axial strain. Zhao et al. (2021) believed

Cite this article as: Zhou B, Zhang E, Dong X, Li C, Li P: Differences in strength, seepage, and acoustic emission characteristics of raw coal and briquette coal samples: A triaxial compression experiment investigation. Acta Geodyn. Geomater., 21, No. 1 (213), 99–110, 2024. DOI: 10.13168/AGG.2024.0009

that the stress-strain curve of raw coal and briquette coal under the local loading has typical stage characteristics. The deformation of raw coal is greater than that of briquette coal at the compaction stage. Briquette coal mainly experiences tensile failure under uniaxial compression, while raw coal mainly experiences type-x shear failure.

Yin et al. (2009) thought the deformation characteristics and compressive strength of briquette coal and raw coal have certain commonalities, but significant differences exist in their mechanical parameters. Briquette coal instead of raw coal is used to study the mechanical properties of coal samples containing gases; raw coal is used to get more realistic mechanical parameters of coal and rocks containing gases. Zhao et al. (2018) considered that the main differences between raw coal and briquette coal exist in the number, size, and complexity of the internal microstructure. Briquette coal instead of raw coal is feasible for mechanical tests; however, it is not suitable for the microscopic observation and analysis of crack evolution. Meng et al. (2020a; 2021b; 2021c) believed that briquette coal supplemented with 7 % of rosin or 20 % of cements is similar to the intensity, deformation, and AE characteristics of raw coal. Although the above studies have obtained the differences in the intensity and seepage of raw coal and briquette coal, the sensitivity analysis of the stress and seepage is lacking.

AE technology is often used to monitor the changes in coal-rock-mass internal fractures (Wang et al., 2019; Zhang et al., 2021). AE signals are generated in the laboratory during the mechanical testing of coal and rock mass (Sun et al., 2019). The amplitude, event number, energy, and other parameters of AE can reflect the number, size, orientation, rupture, expansion, and failure of coal and rock mass. Then the fracture mechanism and fracture of coal and rock mass are identified to predict the related dynamic disaster (Zhang et al., 2018; Zhang et al., 2021). Zhang et al. (2021) concluded that the changes in the AE of raw coal can be divided into a slow growth stage and an accelerated growth stage. Song et al. (2020) explored the microstructure-related AE anisotropy in raw coal. A larger fractal dimension in coal indicates the more uniform distribution of AE counts in the time series and less AE energy consumed during the loading process. Zhou et al. (2022) believed that dynamic-disturbance load accelerates the deformation process of coal samples under the high static pressure. It results in a positive correlation between increased AE characteristic parameters (AE counts and energy) and increased disturbances. Jia et al. (2020) investigated the spatial and temporal evolution of failure in coal at different depths under triaxial compression. The initiation time of failure in coal is accelerated with increasing depth. The failure evolution process is more stable and orderly and ends with higher failure. Kong et al. (2019) selected coal samples in the original cracks for the uniaxial-compression load experiment. The greater initial failure, the lower the uniaxial compressive strength and elastic modulus of coal samples. Most of the above uniaxial AE monitoring tests for coal and rock mass are conducted using raw coal, and the comparative study of briquette coal is missing. Besides, there are few studies on whether the AE evolution law of briquette coal can be used to characterize coal samples under the same external conditions.

Based on above research, the comprehensive comparative analysis is insufficient in the intensity, AE, and seepage characteristics of briquette coal and raw coal. However, the following issues should be discussed, including performance differences between briquette coal and raw coal during the failure process, the experimental results of which coal sample are more congruent with the actual situation, whether the mechanical characteristics of the two types of samples are the same under identical external mechanical conditions, and whether briquette coal accurately reflects the intensity, seepage, and AE characteristics of raw coal.

The triaxial compression experiments of raw coal and briquette coal were performed to analyze their differences in strength, AE response, and seepage characteristics. Their stress sensitivity and gas-permeability velocity sensitivity were further discussed. The results provide an experimental basis for further exploring coal and gas outbursts.

2. MATERIALS AND METHODS

2.1. EXPERIMENTAL MATERIALS

Experimental coal samples were taken from the 9# coal seam of Linhua Mine with high gas content and high pressure. Raw coal was cut, polished, and processed from original coal cores taken from the coal mine by coring equipment. The production of briquette coal was relatively straightforward, involving separate grinding processes for protruding and non-protruding coal. Certain specifications of pulverized coal particles (particle size of 40-60 meshes) mixed uniformly by adding 2 % water in a certain proportion. The molding was formed at 100 MPa using a rigidity tester with a capacity of 2,000 kN. The processed coal sample size was ϕ 50 × 100 mm, and the flatness of both ends was about 0.05 mm. Certain differences existed in surface smoothness and texture among different specimens after the preparation of raw coal and briquette coal. Three samples with the similar density and crack characteristics were separately selected for the two types of coal samples at the beginning of the experiment.

2.2. EXPERIMENTAL SYSTEM AND EXPERIMENTAL PROCEDURE

The experimental setup (Fig. 1) employed a thermos-fluid-structure coupled triaxial servo seepage system for gas-containing coal. It primarily consisted of a gas tank (for applying gas pressure), digital pressure control system (for applying axial and confining pressures), triaxial osmometer, flowmeter,

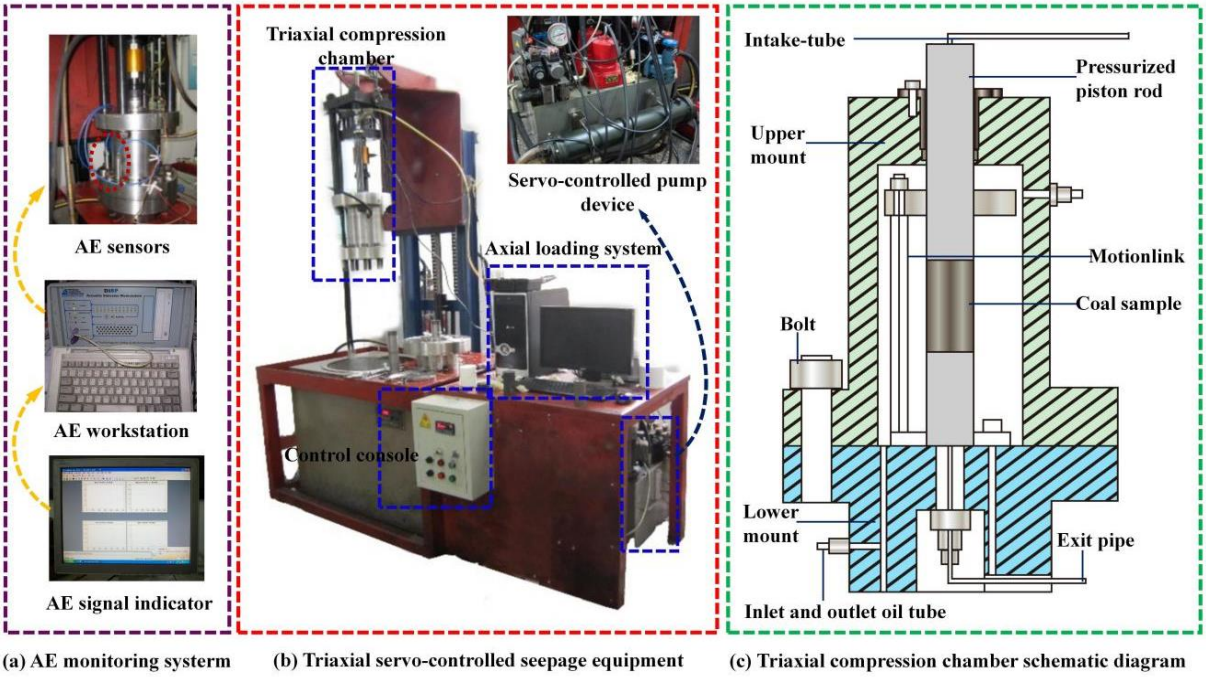

Fig. 1 Experimental facility (Xu et al., 2010).

and computer. The axial pressure was applied by the axial indenter displacement until the sample was damaged. The triaxial compression experiments were performed under a displacement-controlling mode at a loading speed of 0.1 mm/min. Comparative experiments were designed at the gas pressures of 0.5, 1, and 1.5 MPa to investigate the variation law of gas seepage characteristics of briquette coal and raw coal during the stress-strain process of gas-containing coal. The whole process of the seepage experiment was controlled by computers and a control program.

The experiments were conducted using the DS-5 type 8-channel acoustic emission monitoring system to synchronously capture the acoustic emission signals generated during the deformation and failure processes of coal. The acoustic emission monitoring system primarily consisted of acoustic emission sensors, signal amplifiers, and data acquisition hosts. The sampling frequency was 5 MHz, with a waveform threshold of 40 dB. The whole experiment was performed on the control and acquisition platform. All data were collected automatically and continuously by the computer. The gas seepage curves of two types of coal samples and their AE response characteristics in the whole stress-strain process can be obtained according to experimental data.

3. DIFFERENCE ANALYSIS OF STRENGTH CHARACTERISTICS

Figure 2 shows the total stress-strain curves of the two types of coal samples under triaxial compression. Two total stress-strain curves of raw coal and briquette coal have similar changing trends and can be divided into five development stages in the triaxial compression experiment. However, the deformation and failure of the two types of coal samples have obvious differences due to their different structural characteristics. It can be divided into five stages for raw coal: nonlinear compaction stage (stage I), linear elasticity stage (stage II), strain strengthening stage (stage III), stress drop stage (stage IV), and strain softening stage (stage V). The experimental curves of briquette coal can be divided into nonlinear compaction stage (stage I), linear elasticity stage (stage II), yield stage (stage III), strain softening stage (stage IV), and residual load stage (stage V).

Figure 3 shows the changes in the elastic modulus, Poisson's ratio, and axial stress of the two coal samples under triaxial compression. The changing trend of the elastic moduli of raw coal and briquette coal with axial strain is different. The elastic modulus of raw coal shows a trend of a rapid increase, slow increase, and slow decrease with increased axial strain, while the elastic modulus of briquette coal rapidly increases and then remains unchanged. The changing trend of Poisson's ratios of raw coal and briquette coal is the same with increased axial strain–decreasing slowly and then increasing slowly after reaching the minimum.

Comparative analysis shows differences in strength characteristics between two types of coal samples. Firstly, the lateral and axial deformations of briquette coal are about 2-3 times those of raw coal, respectively. Secondly, the compressive strength and elastic modulus of briquette coal are smaller than those of raw coal, and its compressive strength is 66.4 % that of raw coal. The Poisson's ratios of raw coal are 0.62, 0.64, and 0.58, and those of briquette coal are 0.65, 0.85, and 0.85.

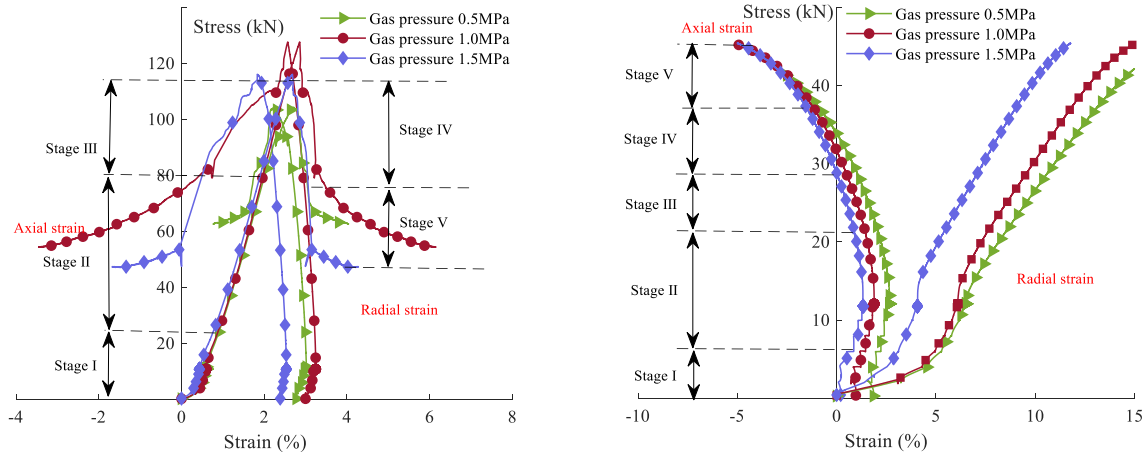

(a) Raw coal samples

(b) Briquette coal samples

Fig. 2 Complete stress-strain curves.

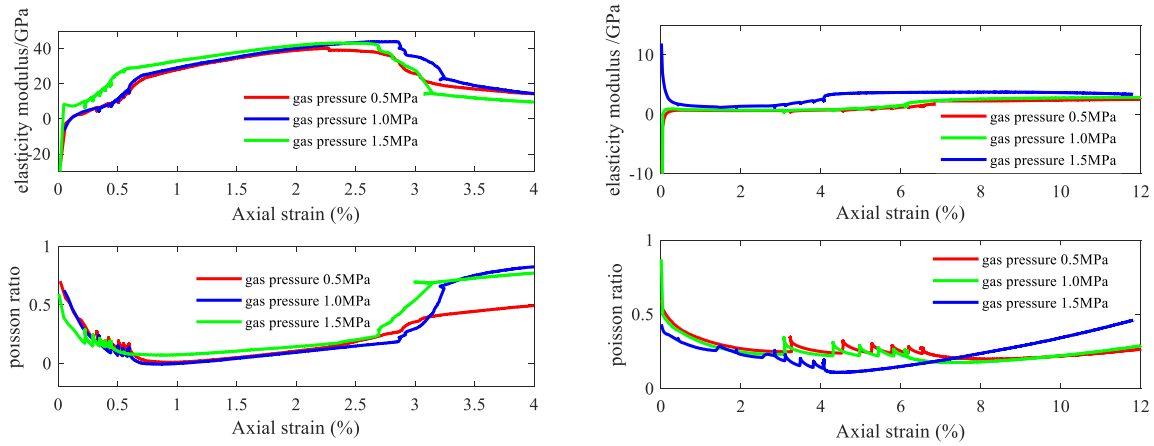

(a) Raw coal samples

(b) Briquette coal samples

Fig. 3 Relationship among the elasticity modulus, Poisson's ratio, and axial strain variation.

The deformation failure stages of the two types of coal samples are different after the peak. Raw coal has stress drops, and the large and rapid change of the axial pressure is consistent with the instantaneous/rapid occurrence characteristics of coal and gas outbursts in the field. Briquette coal mainly reflects strain softening after the peak, with gently decreased axial pressure.

4. DIFFERENTIAL ANALYSIS OF AE CHARACTERISTICS

The AE characterization parameters were analyzed during the fracture of raw coal and briquette coal. Figure 4 shows the eigenvalues and time relationship curves of AE counts and cumulative AE counts in the uniaxial-compression instability and failure of raw coal and briquette coal. Figure 5 presents the curves of the relationship among the AE energy rate, cumulative AE energy, and time.

Figures 4 and 5 show similarities and differences in the AE phenomena between raw coal and briquette coal during triaxial compression. Similarities are as follows: (1) An obvious correspondence exists between AE activity and the stress-strain curve in the instability failure process of triaxial-compression coal samples. It can be roughly divided into five stages as mentioned above. (2) The number of AE events and energy of raw coal and briquette coal is relatively small at stages I and II. When coal samples reach the limit load, they enter stages III and IV. AE counts and AE energy reach the maximum, indicating the precursor of coal-sample failure; (3) AE counts and AE energy gradually decrease during the stress drop process at stage V in AE events.

Differences are mainly manifested in the following aspects: (1) The average AE peak count of raw coal is 62.23 times that of briquette coal, and average AE peak energy is 43.46 times that of

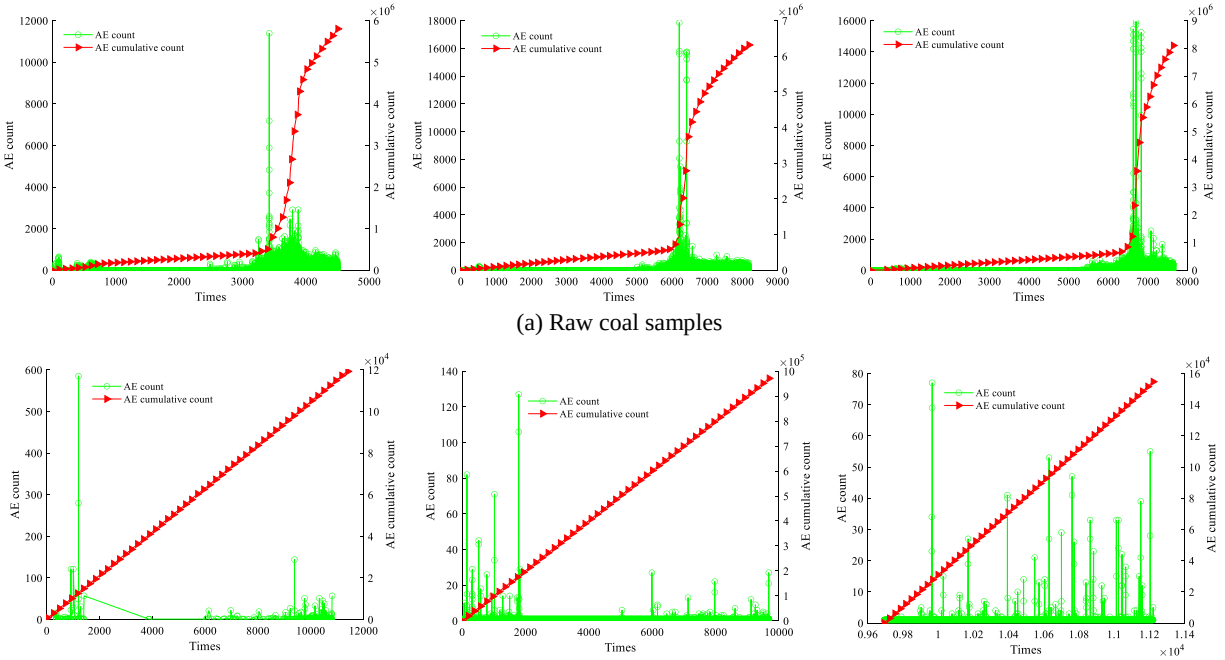

(a) Raw coal samples

(b) Briquette coal samples

Fig. 4 Relationship between AE counts and time variation.

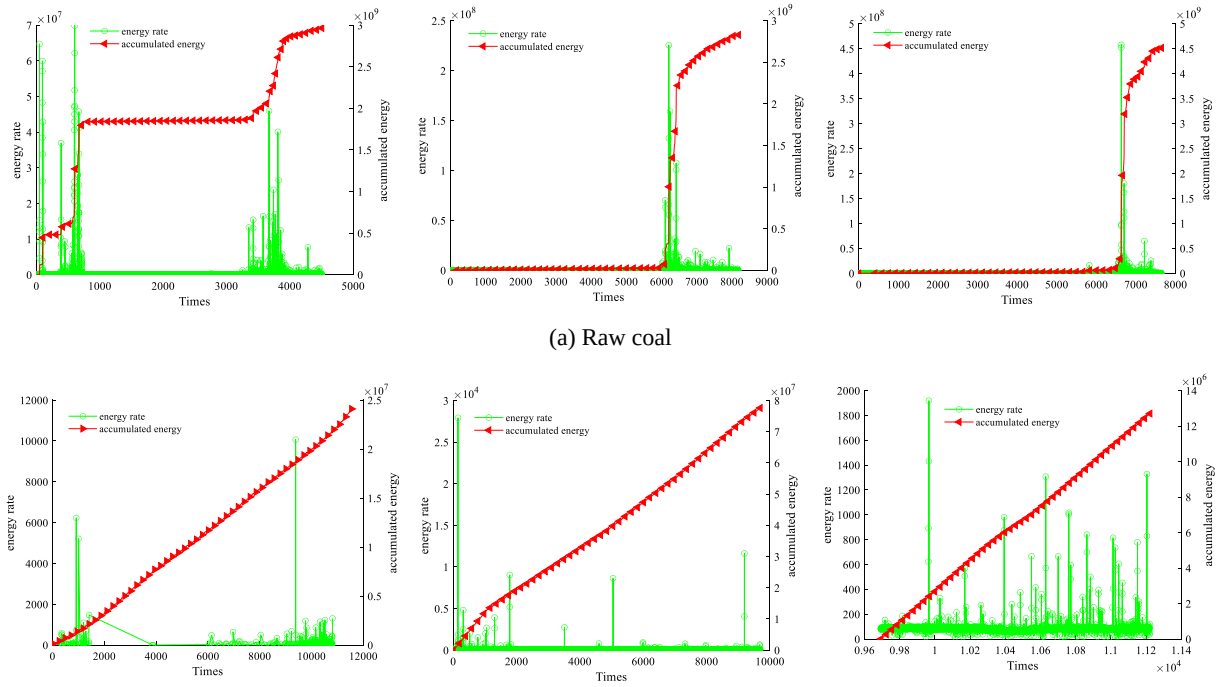

(a) Raw coal

(b) Briquette coal

Fig. 5 Relationship between AE energy and time variation.

briquette coal. The cumulative peak count and energy of raw coal during the whole compression process are higher than those of briquette coal. (2) Original cracks and cavities in raw coal gradually close under the pressure, and almost no new cracks are generated at stages I and II. There are fewer AE events, and the AE source can be considered as the friction between rough contact surfaces in the process of crack closure. Since briquette coal is made of pulverized coal particles and its structure is looser than that of raw coal, the AE event source includes mutual occlusion between particles at stages I and II. Compared with raw coal, the AE-event activity of briquette coal is relatively active. (3) AE events become active at stages III and

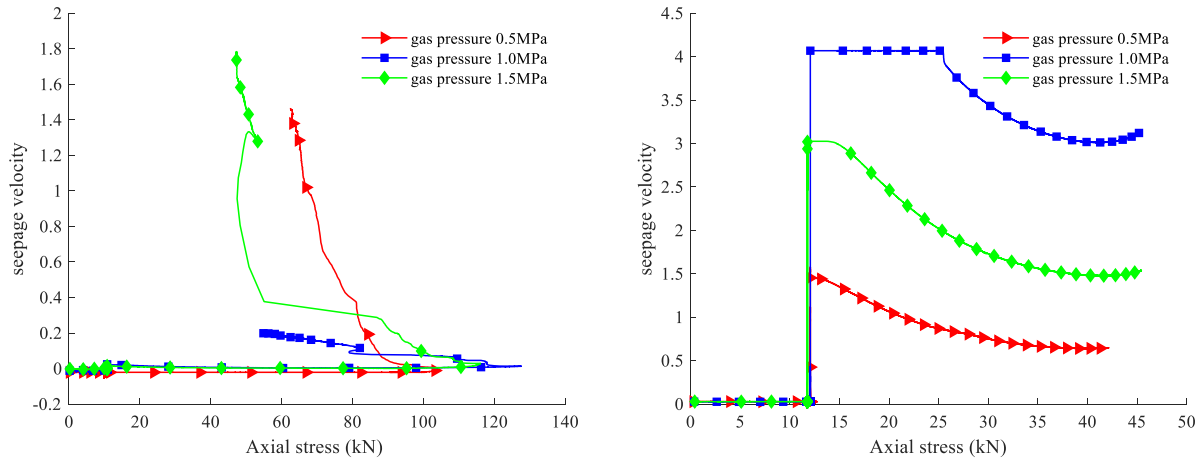

(a) Raw coal samples (b) Briquette coal samples

Fig. 6 Changing curves of the seepage velocity and axial stress.

IV, and AE sources are generated by new fine cracks appearing in coal samples under the high pressure. Large pulverized coal particles break and the internal particles of briquette coal rub and rearrange slowly. The outer walls of coal samples fall off at the initial instability failure stage of briquette coal, which reduces the axial pressure. Raw coal produces a small number of AE events at the early stage. The AE events of raw coal and briquette coal gradually become active at the late plasticity stage, and counts and energy increase greatly. (4) When raw coal reaches its ultimate load, the stress shows a cliff-style drop and AE events decrease rapidly at stage V. The stress decreases after briquette coal reaches its ultimate load, with the residual stress. However, when the stress decreases zigzag, AE events decrease slowly because the outer walls of samples fall off.

5. DIFFERENCE ANALYSIS OF SEEPAGE CHARACTERISTICS

5.1. RELATIONSHIP BETWEEN THE SEEPAGE VELOCITY AND STRESS

Pores and fractures mainly determine the seepage velocities of gases in coal seam. Some original micro pores and micro-cracks exist in raw coal and briquette coal, which is called initial damage. The initial seepage velocity of briquette coal is larger than that of raw coal, indicating that the initial failure of raw coal is much smaller than that of briquette coal. However, initial failure develops and finally connects as the applied load continues to increase, which changes the seepage velocities of gases.

The permeability of briquette coal is 9-70 times that of raw coal under the same experimental conditions. The internal pore volume of briquette coal is much larger than that of raw coal, and the connectivity of pores and fractures is better in briquette coal. While raw coal contains numerous inherent fractures and pore structures, its poor connectivity results in fewer effective gas-flow pathways and lower permeability compared to briquette coal. In contrast, briquette coal is made from coal powder particles with a specific size. Although it has fewer internal fracture structures compared to raw coal, its internal pore structure has better connectivity than raw coal. This results in a larger gas permeation space and higher permeability.

Figure 6 shows the relationship between the seepage velocity and axial stress of two types of coal samples. The variation trend of the seepage velocity of raw coal and briquette coal is the same before the axial stress is less than the yield stress. The velocity decreases with the increased axial pressure and reaches the minimum at the yield-stress point. The difference is that the flow velocity of raw coal and briquette coal decreases by 4.4 and 69.5 % compared with the initial seepage velocity, respectively. Briquette coal is soft, with a lot of voids in the middle and a large compressible space. Although there are primary cracks in raw coal, their original permeability is small and the change is not obvious after compression. When the axial stress is greater than the yield stress, the seepage velocities of the two types of coal samples increase; however, the changing trend is different. The seepage velocity of briquette coal increases smoothly at stage III, while the seepage of fractures occurs in raw coal due to the development of original fractures and the generation of new fractures. Its seepage velocity shows a sudden increase process.

The peak stress point indicates that the samples have reached their maximum bearing capacity. Cracks accumulate before the peak reaches a critical value. Samples are approaching the critical point of complete failure, and the seepage velocity exhibits a distinct inflection point. Stages IV and V reflect seepage velocities after reaching the peak value. The stress decreases rapidly and the seepage velocity increases sharply after reaching the peak stress of raw coal. The main crack of raw coal suddenly generates and expands, with sudden failure. The gas pressure

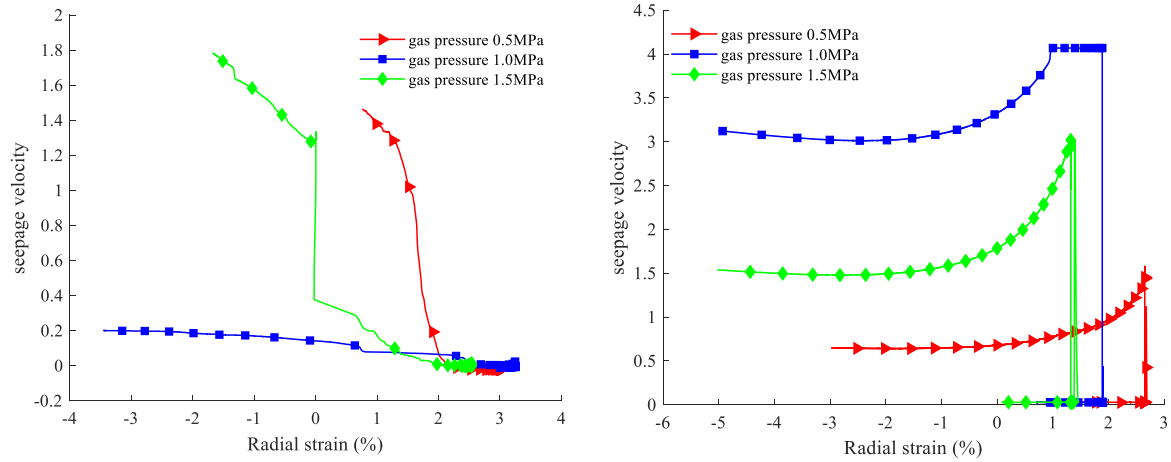

(a) Raw coal samples (b) Briquette coal samples

Fig. 7 Curves of the seepage velocity and radial strain.

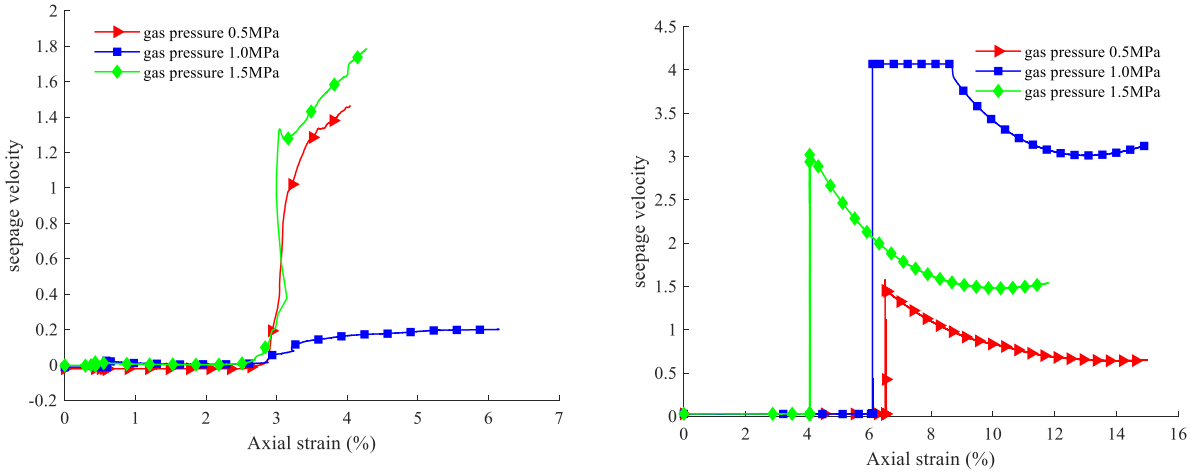

(a) Raw coal samples (b) Briquette coal samples

Fig. 8 Curves of the seepage velocity and axial strain.

gradient increases rapidly after coal is damaged, which increases the risk of coal and gas outbursts. The parameters of briquette coal do not have the suddenness of raw coal (Fig. 6). That is, there are essential differences between briquette coal and raw coal in terms of failure forms and seepage characteristics.

5.2. RELATIONSHIP BETWEEN THE SEEPAGE VELOCITY AND STRAIN

Figueres 7 and 8 show the relationships between the seepage velocity and radial/axial strain of two types of coal samples, respectively. Great differences exist in the variation of gases' seepage velocities.

The stiffness of the two coal samples gradually increases with increased axial compression at stage I of deformation failure. The curve bends upward and the initial defect gradually closes, which corresponds to the nonlinear compaction stage. Meanwhile, the channel for gas flow becomes narrower due to decreased porosity in samples. Then the seepage velocities of raw coal and briquette coal decrease by 7.12 and 7.45 %, respectively.

There is no failure evolution inside raw coal at stage II, and all the original defects only undergo the elastic deformation. Original micropores and microcracks are further closed, but the deformation can be restored after unloading. It corresponds to the linear elastic stage. The seepage velocity of gases decreases by 13.24 % due to the small initial seepage velocity. Pulverized coal particles squeeze and move under the external load of briquette coal. Cohesion decreases and the deformation cannot be recovered after unloading, which corresponds to the linear deformation stage. The original gap between pulverized coal particles is filled, and the seepage velocity of gases drops by 48.45 % rapidly.

The seepage velocities of the two types of coal samples increase at stage III. Shear movement between briquette coal particles induces the expansion of stable cracks under increased strain, which bends the seepage velocity-strain curve. Stiffness decreases, and briquette coal enters the yield deformation stage. Continuous distributed failure occurs inside raw coal, and more and more microcracks develop stably, which results in the plastic deformation. It enters the strain-strengthening stage. The original cracks of raw coal are further developed and new cracks are generated, which increases the seepage velocity of gases by 189.65%. Pulverized coal particles are extruded and undergo shear movement, which results in their separation from samples. New cracks are blocked, so the seepage velocity only increases by 8.45 %.

The largest difference exists in deformation failure between raw coal and briquette coal at stage IV, which reflects the irreplaceability of raw coal. The failure of raw coal progresses from continuous failure to localized failure during the stress drop stage. It results in a sudden reduction of the stress and causes the elastic unloading deformation of original cracks. Inelastic strain borne by the original crack is gradually concentrated into a few cracks produced by localized damage. The rapid release of raw coal's elastic potential energy causes the rapid and violent outburst of coal and gases.

The stress drop is the transition from continuous damage and uniform strain to damage localization and strain localization due to the unstable propagation of cracks. The huge fissure produced by the unstable expansion enables gases to pass through smoothly, and the seepage velocity increases by 90.23 % at the steep-rise stage. Briquette coal is only developed based on the shear failure and the bearing capacity declines, which corresponds to the strain-softening stage. Its internal structure determines that stress drop does not occur suddenly. Therefore, the seepage velocity of briquette coal increases by 31.44 % steadily.

The axial stress of briquette coal remains unchanged at stage V. However, its axial strain gradually increases and coal samples creep, which corresponds to the residual load stage. Although the axial stress is unchanged and samples are compressed axially, the transverse deformation is expanding. The seepage velocity increases by 14.32 %, but the growth trend slows down obviously. Obvious cracks are generated after the failure of raw coal, which results in the stress drop and reduced strength at the strain-softening stage. Some micro-cracks still expand, which raises the seepage velocity of coal samples. The increased rate of the seepage velocity (9.24 %) tends to be gentle.

The analysis of the evolution characteristics of permeability reveals a close relationship between the deformation of coal-rock mass and permeability changes. The relationship between the strain and permeability change of coal exhibits a V-shaped curve, with a decrease in permeability at the high deformation stage and an increase during the low deformation stage. Pores and cracks are compressed at the high deformation stage. The seepage channel is reduced, which blocks gas flow and decreases permeability.

When the pore pressure increases, the compressive deformation of coal samples gradually decreases and the decreasing trend diminishes under the same confining pressure. There is a positive correlation between the coal deformation and permeability at the lower confining pressure. However, when the confining pressure is high, the correlation is not apparent. Despite significant differences in the coal deformation, permeability changes little at the lower confining pressure. In contrast, the opposite is observed at the low deformation stage.

The relationship between strain and permeability follows an exponential equation under the same pore pressure. The strain-permeability changing curve exhibits a critical range. Permeability changes little with variable strain, and the former is highly sensitive to the latter. The coal deformation affects changes in permeability through two main mechanisms: direct action of the confining pressure and pore pressure on the coal deformation and the adsorption-induced deformation due to gas adsorption.

6. DISCUSSION

6.1. STRESS SENSITIVITY ANALYSIS

Permeability damage rate and dimensionless permeability are selected to evaluate the stress sensitivity of coal, and dimensionless permeability K_i/K_0 is defined as the ratio of gas permeability K_i to initial permeability K_0 of samples (Geng et al., 2015). The permeability damage rate reflects the percentage of permeability damage of coal samples under the effective stress, and permeability damage rate D due to stress sensitivity is calculated according to Eq. 1 (Geng et al., 2017; Yan, et al., 2019).

$$D = \frac{K_n - K_{n+1}}{K_n} \times 100\ \% \quad (1)$$

where D is the causeless permeability damage rate generated when the stress increases to the highest point; K_n is the dimensionless permeability of coal samples corresponding to the n^{th} stress point; K_{n+1} is dimensionless permeability at the end of the stage.

Figure 9 shows the experimental results of 6 samples (3 raw coal samples and 3 briquette coal samples). The permeability of raw coal and briquette coal decreases with the increased axial stress according to the negative exponential function. The characteristics are as follows.

(1) The initial permeability of raw coal and briquette coal is different, with an average of 0.029×10^{-3} μm^2 for raw coal and 215.4×10^{-3} μm^2 for briquette coal. However, the variation trend of non-dimensional permeability K_i/K_0 is the same with the increased effective stress (Fig. 9 (a)).

(2) According to the various characteristics of the permeability damage rate with the axial stress in

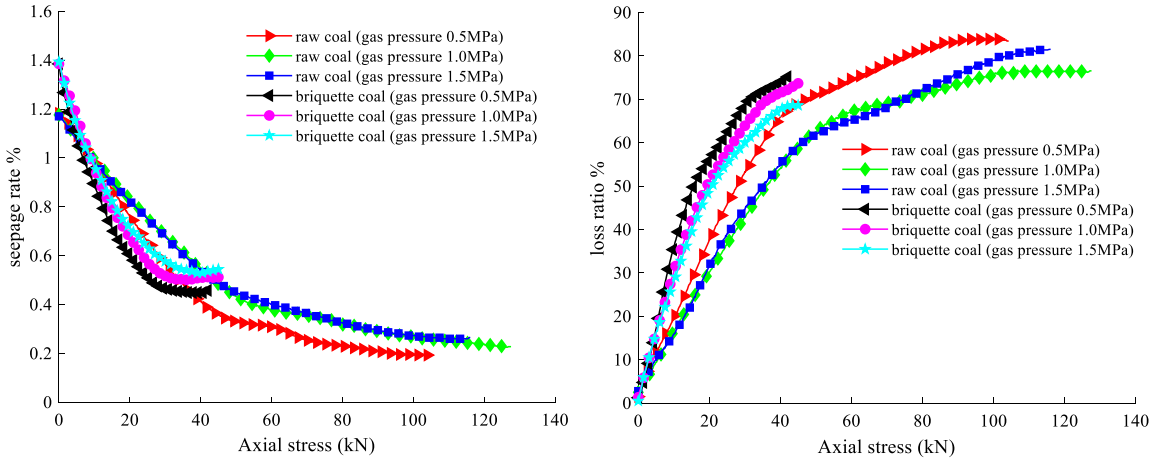

(a) Dimensionless permeability (b) Permeability damage rate

Fig. 9 Variation law of the dimensionless permeability, permeability damage rate, and stress of raw coal and briquette coal.

Figure 9 (b), the dimensionless permeability and permeability damage rate of coal samples change significantly with the increased axial stress in the failure process of gas-containing coal. The non-dimensional permeability of raw coal ranges from 0.22 to 1.18; the damage rate ranges from 0 to 82.12 %, with an average of 40.35 %. The non-dimensional permeability of briquette coal is 0.48-1.37; the damage rate is 0-77.86 %, with an average of 40.54 %. The irreversible permeability of raw coal is slightly higher than that of briquette coal because briquette coal is made of compacted coal particles with no skeleton structure. The seepage channel of briquette coal is mainly a crack in contact with particles. However, microcracks in raw coal are compacted and closed to produce the irreversible plastic deformation. It results in a higher irreversible damage rate after the pressure reduction compared with briquette coal.

(3) The regression analysis of the experimental results shows a negative exponential relationship between the dimensionless permeability of raw coal and briquette coal and the axial stress (Eq. 2).

$$K_i/K_0 = ae^{-b\Delta p} \quad (2)$$

where K_0 is permeability under an initial stress of 3.5 Pa, 10^{-3} μm^2; K_i is permeability under the given stress, 10^{-3} μm^2; a is the fitting parameter; b is the permeability stress-sensitivity factor, MPa^{-1}; Δp is the change in axial stress from the initial condition to a certain stress condition, MPa. Larger b indicates that the sample is more sensitive to the change in axial stress, i.e., the greater change in samples' permeability under the changes of the same magnitude in the axial stress.

Table 1 shows the experimental results of the stress sensitivity of raw coal and briquette coal. The stress sensitivity coefficient of raw coal is 0.11- 0.12 MPa^{-1}, with an average of 0.1133 MPa^{-1}. The stress sensitivity coefficient of briquette coal is 0.10-0.13 MPa^{-1}, with an average of 0.1167 MPa^{-1}. They reflect the strong stress sensitivity of gas-containing coal. Besides, the correlation coefficients of raw coal and briquette are 0.967-0.984 and 0.972- 0.987, respectively. The correlation coefficient of briquette coal is larger than that of raw coal. The curve shows that the permeability of each test point of briquette coal is closer to its fitting curve, while the test point of raw coal deviates greatly from its fitting curve. It is due to the uniform structure of briquette coal as well as the uneven distribution of pores and cracks and the strong heterogeneity of raw coal.

Table 2 shows the stress-sensitivity evaluation parameters of raw coal and briquette coal. The average damage coefficient of raw-coal samples 1-3'

Table 1 Statistical results of stress sensitivity of raw coal and briquette coal.

Sample	Number	Coefficient a	Coefficient b	Correlation coefficient R^2
Raw coal samples	1	1.342	0.11	0.975
	2	1.275	0.12	0.984
	3	1.294	0.11	0.967
Briquette coal samples	4	1.312	0.10	0.987
	5	1.324	0.12	0.975
	6	1.304	0.13	0.972
Average of raw coal samples		1.3037	0.1133	0.9753
Average of briquette coal samples		1.3133	0.1167	0.9780

Table 2 Evaluation parameters of stress sensitivity of raw coal and briquette coal.

Number	η_1/%	η_2/%	S/ MPa^{-1}	η/%		
				Minimum	Maximum	Average
1	70.24	77.56	0.12	0.034	0.175	0.104
2	68.75	73.48	0.11	0.042	0.167	0.112
3	72.68	78.54	0.13	0.051	0.141	0.101
4	58.46	64.38	0.09	0.048	0.124	0.098
5	64.52	69.17	0.10	0.052	0.113	0.097
6	66.98	70.24	0.12	0.049	0.124	0.110
Average of raw coal	70.56	76.53	0.12	0.042	0.161	0.105
Average of briquette coal	63.32	67.93	0.103	0.049	0.12	0.102

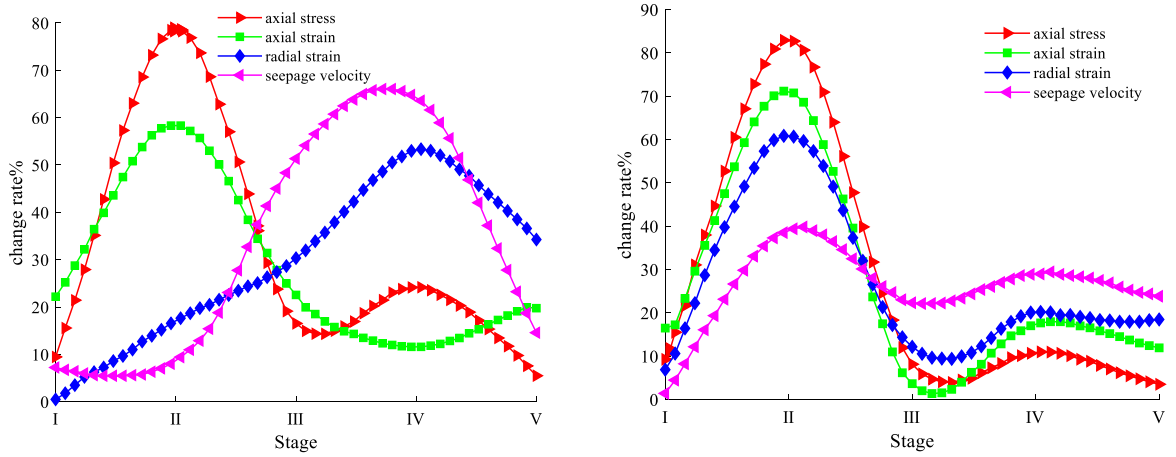

(a) Raw coal samples (b) Briquette coal samples

Fig. 10 Change curves of external conditions and change rates of two types of coal samples.

permeability is 0.042-0.161 MPa^{-1}, with an average of 0.105 MPa^{-1}. The average permeability damage coefficient of briquette coal samples 4-6 is 0.049-0.12 MPa^{-1}, and the average is 0.102 MPa^{-1}. The average stress sensitivity coefficients of raw coal and briquette coal are 0.12 and 0.103 MPa^{-1}, respectively. Their average damage rates are 76.53 and 67.93 % under the maximum axial stress, respectively. These evaluation parameters reflect that both raw coal and briquette coal have strong stress sensitivity, and the permeability damage rate is above 60 % when the axial stress reaches the maximum.

The above analysis shows that the stress-sensitivity evaluation results of raw coal and briquette coal in the 9# coal seam of Linhua Coal Mine are the same. Both have strong stress sensitivity, and their permeability decreases exponentially with the increased axial stress. Therefore, briquette coal can be used as substitutes to study the stress sensitivity of coal reservoirs in the research area where it is difficult to make cylindrical samples.

High-rank coal from a mine in Shanxi has strong stress sensitivity. Therefore, the drainage rate and pressure changes should be strictly controlled in the process of coal-bed gas discharge and mining in this area. Damage to the permeability of coal reservoirs caused by stress sensitivity should be suppressed to avoid stress sensitivity affecting the gas production volume and rate of coal seam.

6.2. SENSITIVITY ANALYSIS OF THE SEEPAGE VELOCITIES OF GASES

External variables, e.g., the axial pressure, confining pressure, axial deformation, radial deformation, and invariant gas pressure in the experiment, affect the seepage velocity of coal samples.

The sensitivity of the seepage velocity of coal samples to the external conditions is analyzed by normalizing the change process of external conditions. The axial deformation and radial deformation are the quantities of increased absolute values, and the maximum value is directly regarded as 1 for normalization. Axial compression and seepage velocity have different change trends in the whole process, and the absolute values of their changes at each stage are summed as 1 for normalization. Figure 10 shows the changing-rate curves of external conditions and the seepage velocities of two types of coal samples.

The changing rate of the seepage velocity has the same change trend as that of external variables for coal

briquette. Especially, it is consistent with the change law of the axial pressure and axial deformation. The changing rates of the seepage velocity, axial pressure, and axial deformation are the largest at the second stage (55, 63, and 73%, respectively); however, those are relatively small at the other stages. The axial stress and deformation of briquette coal have the most obvious influence on the seepage velocity under triaxial compression, that is, the seepage velocity of briquette coal is the most sensitive to axial force and deformation.

Compared with briquette coal, the variation regularity of raw coal variables is less consistent. The variation law of the radial deformation is generally consistent with that of the seepage velocity. The variation range is large at stages III and IV. The radial deformation is the external condition determining the seepage velocity of raw coal, that is, the seepage velocity of raw coal is sensitive to the radial deformation.

7. CONCLUSIONS

The main conclusions are drawn as follows through the comparative study of the deformation, the failure-seepage process of raw coal and briquette coal in the 9# outburst coal seam of Linhua Mine, and the analysis of their AE response characteristics.

(1) The two full stress-strain curves of raw coal and briquette coal had similar trends in the three-axis compression experiment, and they were divided into 5 development stages. The transverse deformation and axial deformation of briquette coal were greater than those of raw coal, and the compressive strength and elastic modulus of briquette coal were less than those of raw coal. The axial stress of raw coal dropped rapidly at the deformation and failure stage, while that of briquette coal decreased slowly.

(2) When coal samples were deformed and damaged, energy reflected by elastic wave signals and accumulated energy increased continuously. However, the AE response characteristics of raw coal and briquette coal were different in the experimental process. The AE event concentration area of raw coal occurred before and after the stress peak of coal-sample failure. The AE response of briquette coal during failure and instability had no obvious characteristics.

(3) The seepage velocity of gases increased with the deformation and failure of coal samples, and its variation trend corresponded to the failure stage of coal samples. The permeability rate of the two was small at the initial stage because of the different cracks and pores in raw coal and briquette coal. However, the maximum permeability velocity of briquette coal was much higher than that of raw coal after coal samples were damaged.

(4) The axial stress and deformation of briquette coal had the most obvious influence on the seepage velocity under triaxial compression. That is, the seepage velocity of briquette coal was the most sensitive to axial force and deformation. The radial deformation was the external condition determining the seepage velocity of raw coal, and the seepage velocity of raw coal was sensitive to the radial deformation.

REFERENCES

Cao, S., Li Y, Guo, P. et al.: 2010, Comparative research on permeability characteristics in complete stress–strain process of briquette coal and coal samples. Chin. J. Rock Mech. Eng., 29, 5, 899–906.

Fu, G., Xie, X., Jia, Q., Tong, W. and Ge, Y.: 2020, Accidents analysis and prevention of coal and gas outburst: Understanding human errors in accidents. Process Saf. Environ. Prot., 134, 1–23. DOI: 10.1016/j.psep.2019.11.026

Ge, L., Yi, F., Du, C., Zhou, J., Cui, Z., Wang, T. et al.: 2022, Deformation localization and damage constitutive model of raw coal and briquette coal under uniaxial compression. Geofluids, 1-2, 1–12. DOI: 10.1155/2022/4922287

Geng, Y., Xu, H., Tang, D. and Tao, S.: 2015, T. Experimental study on stress sensitivity correlation between briquettes and raw coal samples. Coal Sci. Technol., 43, S1, 197–200.

Geng, Y., Tang, D., Xu, H., Tao, S., Tang, S., Ma, L. and Zhu, X.: 2017, Experimental study on permeability stress sensitivity of reconstituted granular coal with different lithotypes. Fuel, 202, 12–22. DOI: 10.1016/j.fuel.2017.03.093

Jia, Z., Xie, H., Zhang, R., Li, C., Wang, M., Gao, M. et al.: 2020, Acoustic emission characteristics and damage evolution of coal at different depths under triaxial compression. Rock Mech. Rock Eng., 53, 5, 2063–76. DOI: 10.1007/s00603-019-02042-w

Kong, X., Wang, E., He, X., Zhao, E. and Zhao, C.: 2019, Mechanical characteristics and dynamic damage evolution mechanism of coal samples in compressive loading experiments. Eng. Fract. Mech., 210, 160–169. DOI: 10.1016/j.engfracmech.2018.04.005

Li, Z., Liu, Z., Mu, C. and Zhang, W.: 2017, Two types of coal samples' dynamic mechanical properties under impact loading. IOP Conf. Ser.: Earth Environ. Sci., 81, 1, 012078. DOI: 10.1088/1755-1315/81/1/012078

Liu, Z., Zhu, D., Yang, H., Wang, W. and Yang, W.: 2022, Experimental research on different metamorphic grades of coal bodies with macro–mesoscopic structure fractal characteristics. Geomech. Energy Envir., 32, 11, 1003372. DOI: 10.1016/j.gete.2022.100337

Christopher, M. and Michael, G.: 2016, Evaluating the risk of coal bursts in underground coal mines. Int. J. Min. Sci. Technol., 26, 1, 47–52. DOI: 10.1016/j.ijmst.2015.11.009

Meng, H., Wu, L., Yang, Y., Wang, F., Peng, L. and Li, L.: 2021, Evolution of mechanical properties and acoustic emission characteristics in uniaxial compression: Raw coal simulation using briquette coal samples with different binders. ACS Omega, 6, 8, 5518–31. DOI:10.1021/acsomega.0c05905

Meng, H., Yang, Y., Wu, L., Wang, F., Peng, L. and Zhang, C.: 2020, Study of strength and deformation evolution in raw and briquette coal samples under uniaxial compression via monitoring their acoustic emission characteristics. Adv. Civ. Eng., 1201, 1–16. DOI: 10.1155/2020/8868754

Meng, H., Yang, Y. and Wu, L.: 2021, Strength, deformation and acoustic emission characteristics of raw coal and briquette coal samples under a triaxial compression experiment. ACS Omega, 6, 47, 31485–98. DOI: 10.1021/acsomega.1c03543

Peng, S.J., Xu, J., Yang, H.W. and Liu, D.: 2012, Experimental study on the influence mechanism of gas seepage on coal and gas outburst disaster. Saf. Sci., 50, 4, 816–21. DOI: 10.1016/j.ssci.2011.08.027

Song, H., Zhao, Y., Elsworth, D., Jiang, Y. and Wang, J.: 2020, Anisotropy of acoustic emission in coal under the uniaxial loading condition. Chaos Solit. Fractals, 130, 109465. DOI: 10.1016/j.chaos.2019.109465

Sun, H., Liu, X.L. and Zhu, J.B.: 2019, Correlational fractal characterisation of stress and acoustic emission during9 coal and rock failure under multilevel dynamic loading. Int. J. Rock Mech. Min. Sci., 117, 1–10. DOI: 10.1016/j.ijrmms.2019.03.002

Wang, H.L., Song, D.Z., Li, Z.L., Hem X.Q., Lan, S.R. and Guo, H.F.: 2020, Acoustic emission characteristics of coal failure using automatic speech recognition methodology analysis. Int. J. Rock Mech. Min. Sci., 136, 104472. DOI: 10.1016/j.ijrmms.2020.104472

Wang, W., Wang, H., Zhang, B., Wang, S. and Xing, W.: 2021, Coal and gas outburst prediction model based on extension theory and its application. Process Saf. Environ. Prot., 154, 329–37. DOI: 10.1016/j.psep.2021.08.023

Wang, Z.L., Hao, S.Y., Zheng, J., Tian, N.C., Zha, F.S. and Shi, H.: 2019, Study on energy properties and failure behaviors of heat–treated granite under static and dynamic compression. Mech. Adv. Mater. Struct., 27, 6, 462–72. DOI: 10.1080/15376494.2018.1479808

Wei, X., Gao, M., Lv, Y., Shi, X., Gao, H. and Zhou, H.: 2012, Evolution of a mining induced fracture network in the overburden strata of an inclined coal seam. Int. J. Min. Sci. Technol., 22, 6, 779–83. DOI: 10.1016/j.ijmst.2012.11.004

Wu, Y., Gao, R. and Yang, J.: 2020, Prediction of coal and gas outburst: a method based on the BP neural network optimized by GASA. Process Saf. Environ. Prot., 133, 64–72. DOI: 10.1016/j.psep.2019.10.002

Xu, J., Peng, S., Yin, G., Tao, Y., Yang, H. and Wang, W.: 2010, Development and application of triaxial servocontrolled seepage equipment for thermo–fluid–solid coupling of coal containing methane. Chin. J. Rock Mech. Eng., 29, 5, 907–914.

Yan, Z., Wang, K., Zang, J., Wang, C. and Liu, A.: 2019, Anisotropic coal permeability and its stress sensitivity. Int. J. Min. Sci. Technol., 29, 3, 507–511. DOI: 10.1016/j.ijmst.2018.10.005

Yin, G., Wang, D., Zhang, D. et al.: 2009, Test analysis of deformation characteristics and compressive strengths of two types of coal specimens containing gas. Chin. J. Rock Mech. Eng., 28, 2, 410–417.

Zhang, H., Zhao, H., Li, W., Yang, X. and Wang, T.: 2020, Influence of local frequent dynamic disturbance on micro–structure evolution of coal–rock and localization effect. Nat. Resour. Res., 29, 6, 3917–42. DOI: 10.1007/s11053-020-09683-7

Zhang, J., Ai, C., Li, Y-W., Che, M-G., Gao, R. and Zeng, J.: 2018, Energy-based brittleness index and acoustic emission characteristics of anisotropic coal under triaxial stress condition. Rock Mech. Rock Eng., 51, 11, 3343–60. DOI: 10.1007/s00603-018-1535-9

Zhang, L., Ren, T., Li, X. and Tan, L.: 2021, Acoustic emission, damage and cracking evolution of intact coal under compressive loads: Experimental and discrete element modelling. Eng. Fract. Mech., 252, 107690. DOI: 10.1016/j.engfracmech.2021.107690

Zhang, R., Liu, J., Sa, Z., Wang, Z. and Lu, S. and Lv, Z.: 2021, Fractal characteristics of acoustic emission of gas-bearing coal subjected to true triaxial loading. Measurement, 169, 108349. DOI: 10.1016/j.measurement.2020.108349

Zhang, Z., Liu, X., Zhang, Y., Qin, X. and Khan, M.: 2021, Comparative study on fracture characteristics of coal and rock samples based on acoustic emission technology. Theor. Appl. Fract. Mech., 111, 102851. DOI: 10.1016/j.tafmec.2020.102851

Zhang, E., Zhou, B., Yang, L., Li, C. and Li, P.: 2023, Experimental study on the microseismic response characteristics of coal and gas outbursts. Process Saf. Environ. Prot., 172, 1058–1071. DOI: 10.1016/j.psep.2023.02.089

Zhao, H., Wang, T., Li, J., Liu, Y. and Su, B.: 2021, Regional characteristics of deformation and failure of coal and rock under local loading. J. Test. Eval., 49, 5, 3701–15. DOI: 10.1520/JTE20190881

Zhao, H, Wang, T., Zhang, H. and Wei, Z.: 2018, Comparison of local load influence on crack evolution of coal and briquette coal samples. Adv. Civ. Eng., 1790785. DOI: 10.1155/2018/1790785

Zhou, A., Du, Ch., Wang, K., Hu, J. and Fan, X.: 2022, Experimental research on the law of the deformation and damage characteristics of raw coal/ briquette adsorption–instantaneous pressure relief. Fuel, 308, 6, 122062. DOI: 10.1016/j.fuel.2021.122062

Zhou, X., Liu, X., Wang, X., Liu, Y., Xie, H. and Du, P.: 2022, Acoustic emission characteristics of coal failure under triaxial loading and unloading disturbance. Rock Mech. Rock Eng., 56, 2, 1043–61. DOI: 10.1007/s00603-022-03104-2